ISOSTRUCTURAL MOTT TRANSITION IN 2D HONEYCOMB ANTIFERROMAGNET $V_{0.9}PS_3$ - SUPPLEMENTARY INFORMATION

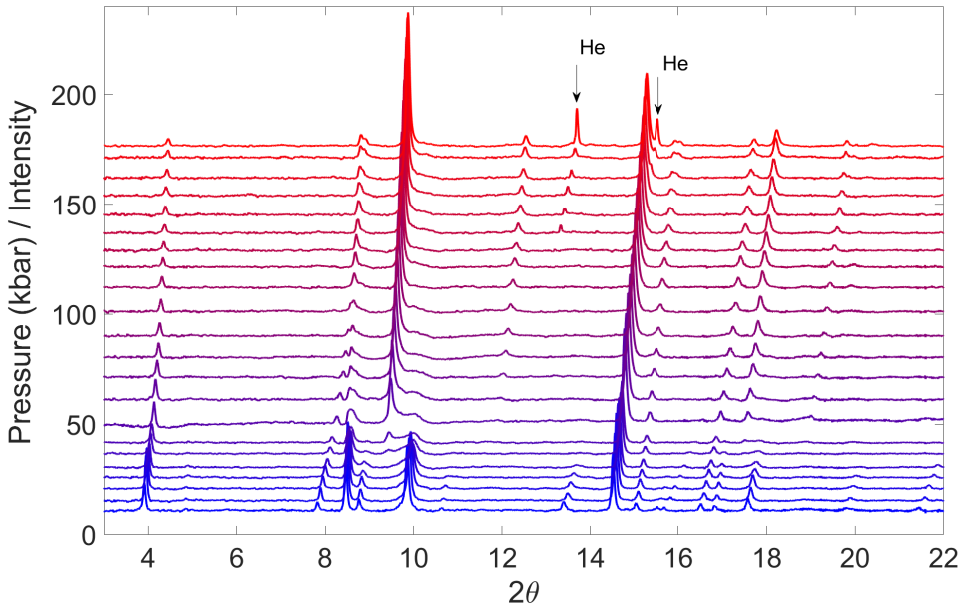

Figure 1. Integrated powder diffraction patterns for $V_{0.9}PS_3$ at room temperature. A diffuse background has been subtracted and the y-axis offset of each curve has been set to the value of its pressure in kbar.

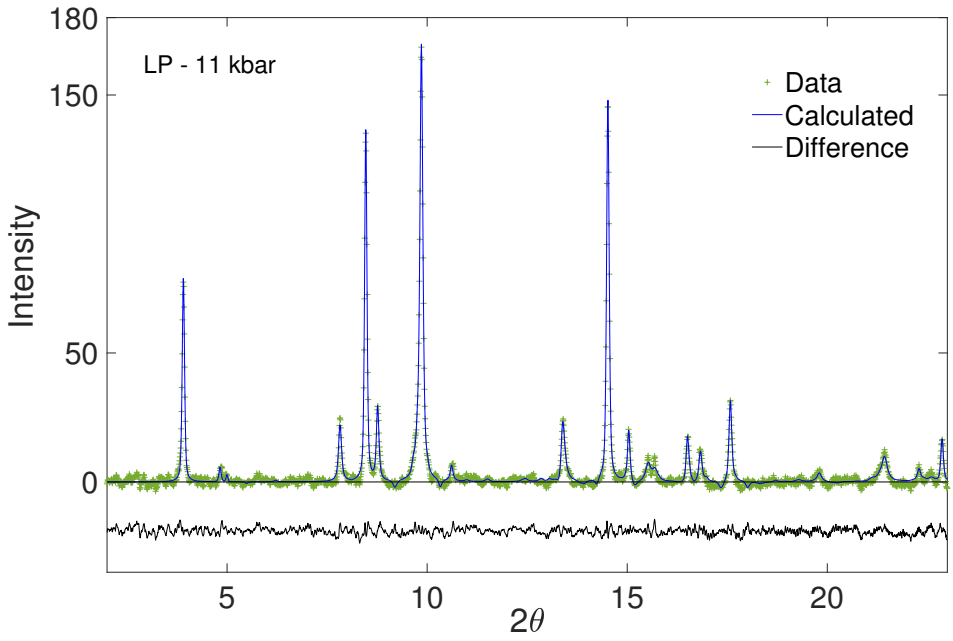

Figure 2. Rietveld refinement of the integrated powder x-ray patterns, after subtraction of a diffuse background, for $V_{0.9}PS_3$ at 11 kbar (the lowest pressure measured), in the LP phase.

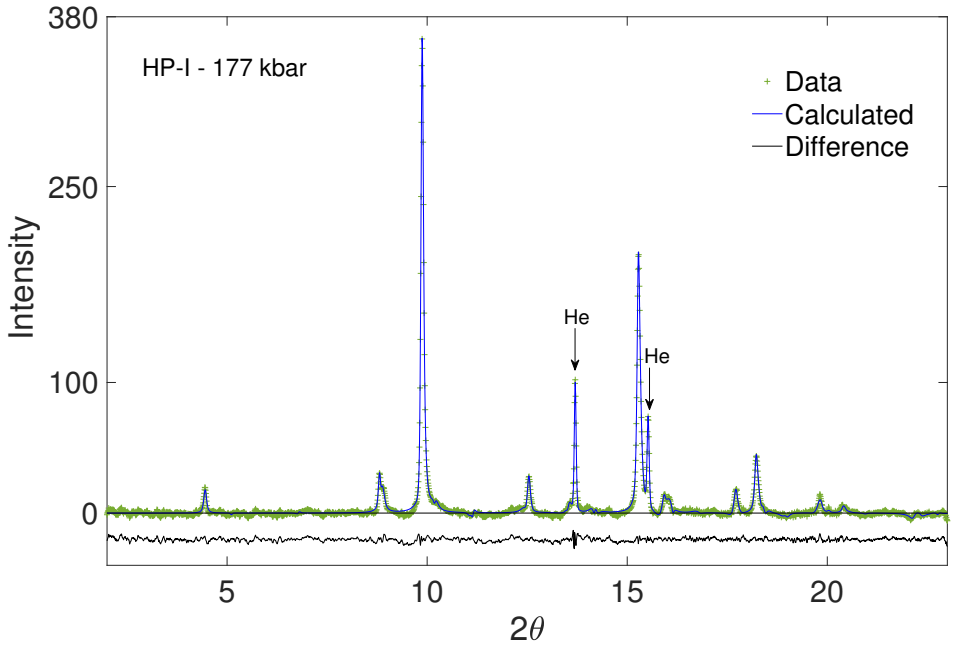

Figure 3. Rietveld refinement of the integrated powder x-ray patterns, after subtraction of a diffuse background, for $V_{0.9}PS_3$ at 177 kbar, in the HP-I phase. The peaks marked 'He' in are due to the solid helium pressure medium and were included in the refinement as an additional phase or impurity. These appear at 150 kbar - the freezing point of helium at room temperature, and the change of their positions with pressure were found to match the data of Mao et.al. [1].

LP (11 kbar)	C2/m	$R = 7\%$	$wR = 9\%$	$\chi^2 = 3.01$	GOF = 4%
$a = 5.8436(15)$ Å	$b = 10.0876(8)$ Å	$c = 6.5237(18)$ Å	$\beta = 107.098(5)$ º	V = 367.56(6) Å^3	$\rho = 3.060(1)$ g.cm^{-3}

	x	y	z	Occ	U_{iso}
V(4g)	0	0.331(1)	0	0.86(4)	0.079(4)
P(4i)	0.043(4)	0	0.122(3)	1	0.091(6)
S(4i)	0.758(2)	0	0.249(4)	1	0.071(6)
S(8j)	0.260(2)	0.1738(7)	0.234(2)	1	0.070(3)

HP-I (177 kbar)	C2/m	$R = 7\%$	$wR = 10\%$	$\chi^2 = 3.56$	GOF = 4%
$a = 5.5469(3)$ Å	$b = 9.5892(6)$ Å	$c = 5.4788(9)$ Å	$\beta = 90.136(8)$ º	V = 291.42(7) Å^3	$\rho = 3.813(1)$ g.cm^{-3}

	x	y	z	Occ	U_{iso}
V(4g)	0	0.3431(4)	0	0.86(4)	0.090(3)
P(4i)	0.0076(7)	0	0.8492(20)	1	0.061(3)
S(4i)	0.3257(11)	0	0.7214(7)	1	0.025(4)
S(8j)	0.8441(3)	0.1649(3)	0.7510(5)	1	0.039(3)

Table I. Refinement parameters for the LP low-pressure phase at 11 kbar and the HP-I high-pressure phase at 177 kbar.

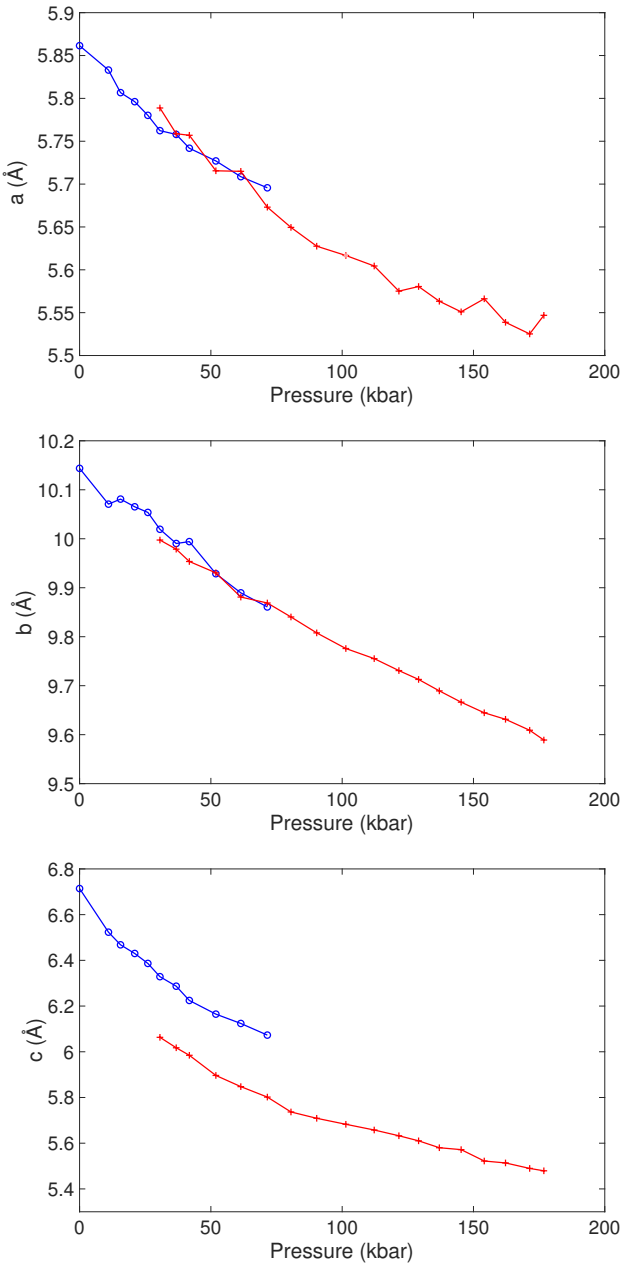

Figure 4. Lattice parameters extracted from powder x-ray refinements for $V_{0.9}PS_3$ at room temperature as a function of pressure. Blue circles denote the LP phase and red crosses the HP-I phase. Note that while there is a jump in the c axis value between the two phases, this is due to a change in β and does not correspond to a change in inter-planar spacing or cell volume.

Figure 5. Photograph of the diamond anvil cell sample region and gasket, installed on the lower anvil prior to loading of the pressure medium and pressurization. The four gold wires connected to the single-crystal $V_{0.9}PS_3$ crystal can be seen running along insulated epoxy tracks dug into the Be-Cu gasket. Two ruby chips are visible above and to the right of the sample.

a)

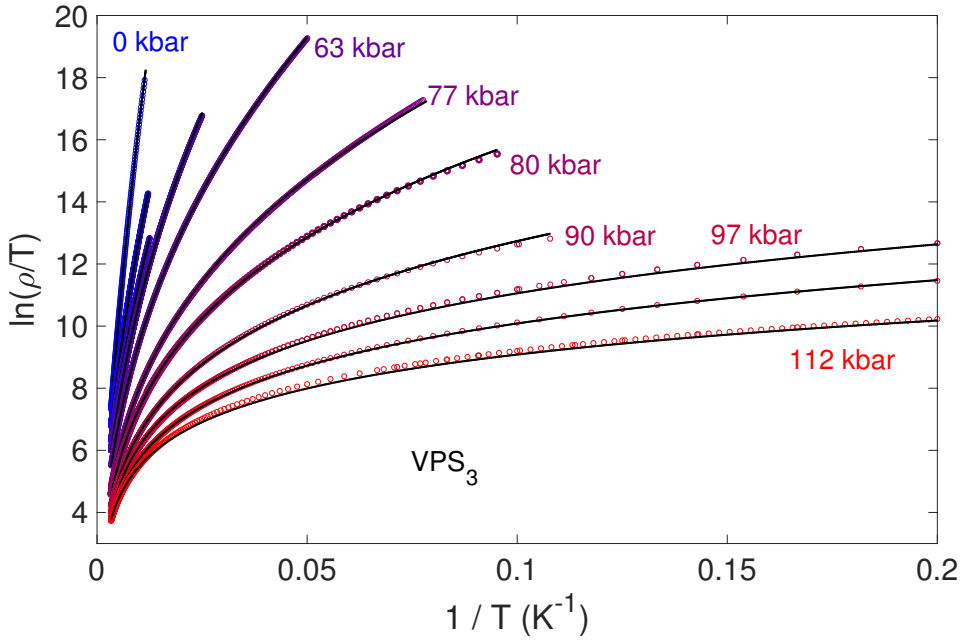

b)

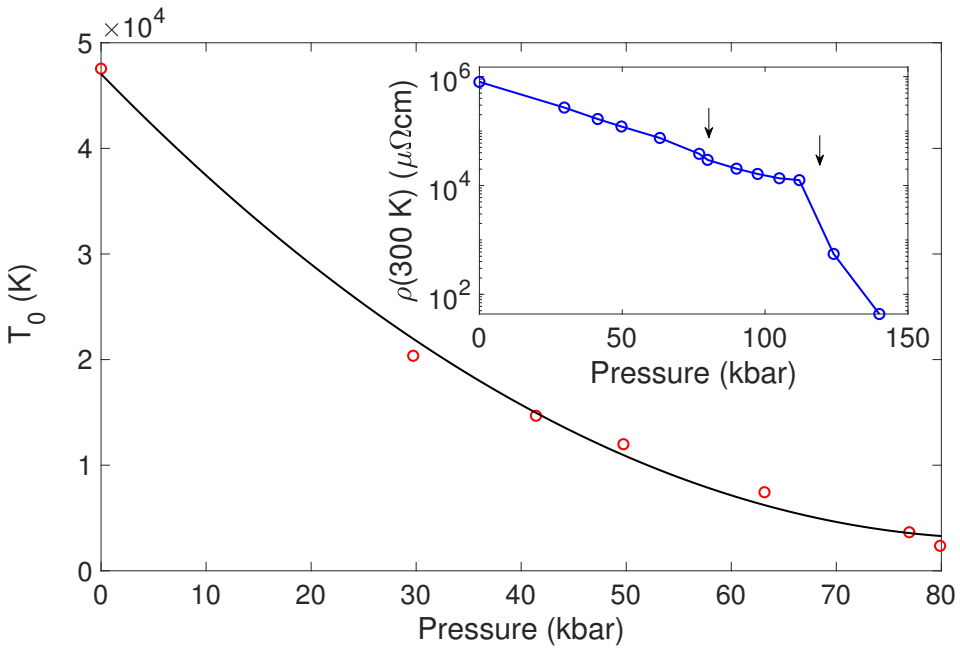

Figure 6. a) - $\ln(\rho/T)$ vs $1/T$ plotted to extract the α power law dependence in the generalized variable range hopping expression discussed in the main text $\rho = \rho_0 T e^{(T_0/T)^\alpha}$. Fits of type $1/T^\alpha$ are shown as black lines, allowing the exponent α to be extracted. b) - extracted values of the T_0 characteristic temperature. Inset shows values of the room-temperature resistivity as pressure is increased, on a logarithmic axis. Arrows denote a kink or change of slope at 80 kbar and the insulator-metal transition between 112-124 kbar.

Unlike in other MPX_3 materials such as $FePS_3$ [2], the resistivity cannot be well described by a simple Arrhenius-type insulating temperature dependence - Fig. 6.a illustrates this by plotting $\ln(\rho/T)$ against $1/T$ - the resulting plots are far from straight lines and can be fitted with a simple power law dependence. The simpler form $\ln(\rho)$ against $1/T$ for an equivalent plot gives an extremely similar result and is the standard test for Arrhenius e^{E_a/k_bT} resistivity. Fig. 6.b shows the extracted characteristic temperature T_0 and the room temperature resistivity. If the

data follows variable-range-hopping expression $\rho = \rho_0 T e^{(T_0/T)^\alpha}$, plotting $\ln(\rho/T)$ against $1/T$ as in Fig. 6.a then yields an expression $\ln(\rho/T) = \ln(\rho_0) + T_0^\alpha (1/T)^\alpha$ and so the exponent α can easily be found from a non-linear least-squares fit. Such fits are shown overlayed onto the data curves - good fits are seen up to pressures around 80 kbar, but then the quality of fits starts to decrease as the data move away from the VRH form, particularly at lower temperatures, as the insulator-metal transition is approached.

As the transition is approached, the T_o characteristic temperature is continuously suppressed - again, no clear abrupt changes - until the VRH expression breaks down in the close proximity of metallization above 80 kbar. As electron overlap is increased by pressure, the hopping energies are gradually decreasing. The decrease in the room-temperature resistivity - a metric which is of course independent of any fitting methodology - is once again smooth and continuous, except for the insulator-metal transition at 112-124 kbar and a slight kink or change of slope around 80 kbar. 80 kbar corresponds to the maximum pressure of the LP - HP-I structural crossover, so a change in $\rho(p)$ can be expected here as phase ratios are no longer changing and affecting the resistivity.

[1] H. Mao, R. Hemley, Y. Wu, A. Jephcoat, L. Finger, C. Zha, and W. Bassett, Physical Review Letters **60**, 2649 (1988).
[2] C. Haines, M. Coak, A. Wildes, G. Lampronti, C. Liu, P. Nahai-Williamson, H. Hamidov, D. Daisenberger, and S. Saxena, Physical Review Letters **121** (2018), 10.1103/physrevlett.121.266801.